nature neuroscience

Attention-dependent reductions in burstiness and action-potential height in macaque area V4

Emily B Anderson[1,2], Jude F Mitchell[1] & John H Reynolds[1]

Attention improves the encoding of visual stimuli. One mechanism that is implicated in facilitating sensory encoding is the firing of action potentials in bursts. We tested the hypothesis that when spatial attention is directed to a stimulus, this causes an increase in burst firing to the attended stimulus. To the contrary, we found an attention-dependent reduction in 'burstiness' among putative pyramidal neurons in macaque area V4. We accounted for this using a conductance-based Hodgkin-Huxley style model in which attentional modulation stems from scaling excitation and inhibition. The model exhibited attention-dependent increases in firing rate and made the surprising and correct prediction that when attention is directed into a neuron's receptive field, this reduces action-potential height. The model thus provided a unified explanation for three distinct forms of attentional modulation, two of them previously undescribed, and implicates scaling of the responses of excitatory and inhibitory input populations in mediating attention.

The role of burst firing in sensory processing is unknown. Previous studies have argued that bursts may have a privileged role in sensory encoding, as they have been shown to carry sensory information and propagate more reliably than individual action potentials[1]. In the thalamus, neurons in burst mode exhibit greater sensitivity to incoming stimuli, whereas nonbursting responses are more graded and exhibit better linear summation[2]. In primary visual and auditory cortex, bursts of action potentials exhibit sharper tuning to stimulus features than isolated spikes[3–5] and make a larger contribution to receptive field (RF) properties[6]. Burst firing in cortex may also have a central role in selective communication[7] and in regulation of synaptic integration and plasticity[8,9]. Studies in the zebra finch song system and the pyramidal neurons of the weakly electric fish have provided evidence that burst firing has a role in detecting highly specific, behaviorally relevant events[1].

If burst firing is important for encoding and transmission of sensory information, then burst rate might be expected to increase when attention is directed to a stimulus. To test this hypothesis, we recorded responses in macaque area V4, an intermediate stage of processing in the ventral visual processing stream, which previous lesion studies and single unit recording studies have implicated in selective attention[10,11]. We compared the propensity of neurons to fire bursts of action potentials ('burstiness') when attention was directed into or away from their RFs. Contrary to the hypothesis that burst firing should increase with attention, we found that it was reduced.

We describe a conductance-based Hodgkin-Huxley style neuron model that accounts for both the attention-dependent increases in rate previously reported as well as the reductions in burst firing observed in the current study. The model also predicted that the height of action potentials should decrease with attention. We found an attention-dependent reduction in action-potential height that was comparable to the reductions predicted by the model. Taken together, the present findings show that attention reduces burst firing and spike height, and suggests that attentional modulation depends on a relatively simple mechanism: an attention-dependent increase in excitatory and inhibitory synaptic conductance.

RESULTS

Attention-dependent reduction in burstiness

To investigate the role of burst firing in macaque area V4, we compared the burstiness of neural responses when attention was directed to or away from individual neurons' RFs, using an attention-demanding tracking task. V4 neurons can be separated into narrow-spiking and broad-spiking categories, corresponding to putative fast-spiking interneurons and pyramidal neurons[12]. We use the term 'putative' here because the relationship between spiking width and cell class identity is not one to one. A small fraction of neurons (10–15%) are broad-spiking interneurons, and several studies have found examples of narrow-spiking pyramidal neurons[13–15].

Consistent with *in vitro* physiology, putative pyramidal neurons exhibit a much larger degree of burst spiking, often firing doublets and triplets of spikes at short interspike intervals (ISIs)[16]. In **Figure 1**, we show two example broad-spiking (putative pyramidal) neurons that exhibited an attention-dependent reduction in burstiness. Both neurons exhibited a robust increase in firing rate with attention. The mean firing rate of the first neuron increased from 36.2 Hz to 48.4 Hz (33.6% increase with attention directed into the RF), and the mean firing rate of the second neuron of the increased from 7.1 Hz to 12.1 Hz (69.8% increase).

To quantify the degree of burst firing across the two attention conditions, we examined ISI distributions of each neuron (**Fig. 1a**,**b**). We hypothesized that if burst firing were critical for sensory encoding,

[1]The Salk Institute for Biological Studies, San Diego, California, USA. [2]Center for Integrative Neuroscience and Department of Physiology, University of California, San Francisco, San Francisco, California, USA. Correspondence should be addressed to J.H.R. (reynolds@salk.edu) or E.B.A. (emily@phy.ucsf.edu).

Received 16 January; accepted 12 June; published online 14 July 2013; corrected online 17 July 2013 (details online); doi:10.1038/nn.3463

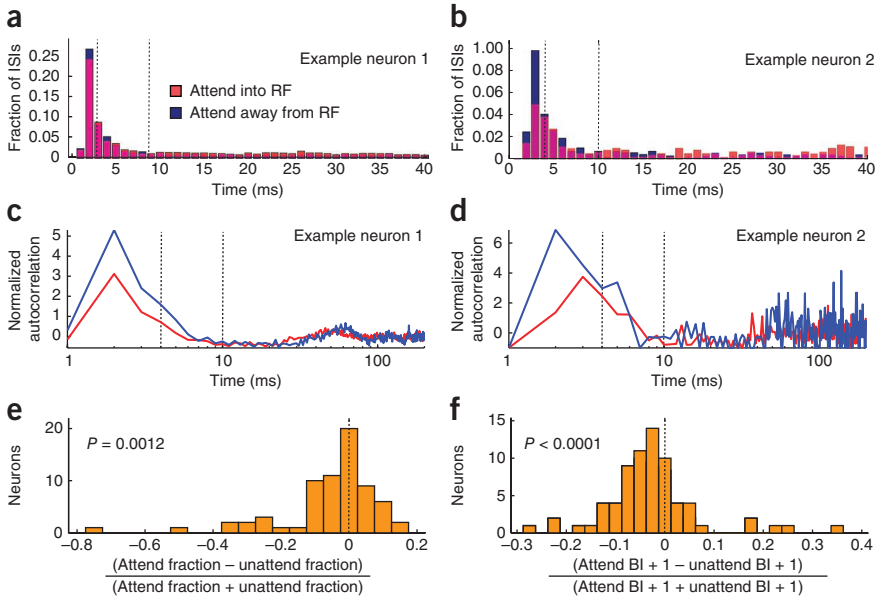

Figure 1 Attention-dependent reduction in the burstiness. (**a**,**b**) ISI histogram for two example neurons, with the two attention conditions superimposed. Note the higher fraction of short ISIs among the unattended trials. (**c**,**d**) Attention-dependent reduction of the normalized autocorrelation function at short time lags (log scale) for the neurons in **a** and **b**, respectively. Note the reduction in the peak of the autocorrelation function in the attended condition relative to the unattended condition, indicative of a reduction in burst firing. (**e**) Changes in burst fraction (ISI < 4 ms), normalized by sum, among 69 broad-spiking neurons, indicating significant attention-dependent reduction in the fraction of action potentials in bursts with attention. (Two units did not have ISIs < 4 ms in either attention condition.) (**f**) Changes in burst index (BI), normalized by sum, also indicating significant attention-dependent reduction in burst fraction with attention ($n = 71$).

we would see an attention-dependent increase in burstiness, which we could measure as an increase in the percentage of short ISIs. Contrary to this prediction, we found an attention-dependent reduction in the proportion of short ISIs (<4 ms) for both of our example neurons, reflecting a reduction in the proportion of burst events. Despite the increase in firing rate, which would be expected to result in an increase in the fraction of short ISIs, both neurons exhibited reductions in the fraction of short ISIs with attention.

We quantified the fraction of short ISIs across the broad-spiking population and found a systematic reduction in this measure of burst firing when attention was directed into the neurons' RFs. These neurons had a significantly higher percentage of short ISIs in the unattended condition, indicating a reduction in burstiness with attention (Wilcoxon signed-rank test, $P = 0.00097$, $n = 71$). We did not observe a significant reduction in burstiness among narrow-spiking neurons ($P = 0.20$, $n = 47$). For each neuron, we also computed a burst attention modulation index, which was the difference in the percentage of ISIs less than 4 ms across the two attention conditions, normalized by their sum. Broad-spiking neurons exhibited a significant reduction in this burst index (Wilcoxon signed-rank test, $P = 0.0012$, **Fig. 1e**; see **Supplementary Fig. 1a**). This reduction tended to occur among neurons with lower firing rates (**Supplementary Fig. 2**). In contrast, we did not see a significant reduction among narrow-spiking neurons (Wilcoxon signed-rank test, $P = 0.61$). The difference between burst attention modulation index distributions of the two populations was significant (Mann-Whitney U test, $P = 0.025$).

Slow fluctuations in firing rate are an important source of the variability in the V4 sustained response[17] that may reflect a more general feature of cortical activity[18,19]. These slow fluctuations are reduced by attention[17]. To rule out the possibility that the observed reduction in burst firing might be an artifact of this attention-dependent reduction in low-frequency fluctuations, we developed a second, autocorrelation-based burst metric. This metric subtracted out the effects of low-frequency fluctuations, thereby isolating the contribution of burst firing events at short delays from longer-timescale fluctuations (Online Methods). As with the ISI-based burst metric, the majority of broad-spiking neurons exhibited reductions in this index (Wilcoxon signed-rank test, $P < 0.0001$, **Fig. 1f**; see also **Supplementary Fig. 1b**). We again found no evidence for changes in burst firing with attention among narrow-spiking neurons ($P = 0.67$). Reductions in burstiness were significant among broad-spiking neurons collected in each individual monkey, using either metric ($P < 0.05$). Neither monkey's narrow-spiking neurons showed significant modulation of burstiness using either metric ($P > 0.05$, Wilcoxon signed-rank test).

This reduction in burstiness among broad-spiking, but not narrow-spiking neuron population may reflect a cell type–specific difference in attentional modulation of burst firing. However, narrow-spiking neurons do not tend to fire bursts of action potentials, limiting our ability to observe a reduction in burstiness. Furthermore, the mean firing rate among narrow-spiking neurons was greater than among broad-spiking neurons, making it difficult to rule out that differences between classes stem from differences in their mean rate. Across the combined population of narrow-spiking and broad-spiking neurons, we observed a significant reduction in burstiness with either burstiness metric (Wilcoxon signed-rank test, $P < 0.05$).

The scaled conductance model of attention

Cortical pyramidal neurons exhibit less burstiness in response to depolarization[20] and during the transition from sleep to quiet wakefulness[21]. This suggests that the attention-dependent reductions in burstiness we observed could potentially result from an attention-dependent increase in neuronal depolarization. To formalize this, we developed a conductance-based Hodgkin-Huxley–style model that exhibited burst spiking and evaluated how attention-dependent increases in synaptic activity, resulting in increased mean depolarization, might modulate its burst firing.

The scaled conductance model of attention (**Fig. 2a**) is based on a single-compartment model of burst firing in CA1 pyramidal neurons[22]. The model includes several active conductance channels, including Hodgkin-Huxley–type voltage-dependent conductances that drive action potentials as well as several calcium-dependent channels that regulate after hyperpolarization and spike adaptation. The model includes muscarinic potassium channels and persistent sodium channels that contribute to burst spiking. Previous work examined in detail the role of these two channels in modulating bursting activity in pyramidal neurons[22].

We incorporated attention-dependent changes in synaptic input to examine how this modulates burst firing. We modeled synaptic inputs

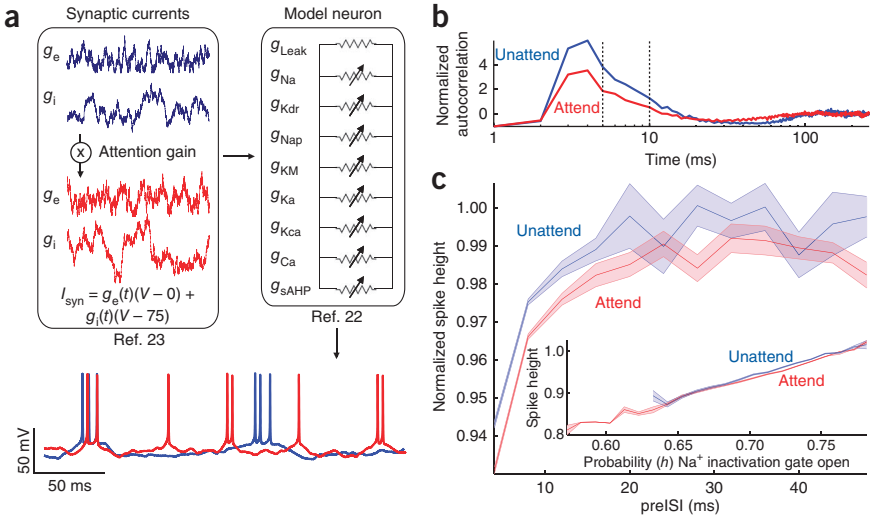

Figure 2 Scaled conductance model of attention. (**a**) Schematic of model neuron (right) and fluctuating synaptic inputs (left), and example intracellular traces produced by the model in the attended (red) and unattended (blue) conditions (bottom). g_{Leak}, leak conductance; g_{Na}, transient Na^+ conductance; g_{Kdr}, delayed rectified K^+ conductance; g_{Nap}, persistent sodium conductance; g_{KM}, muscarinic K^+ conductance; g_{Ka}, A-type K^+ conductance; g_{Kca}, fast Ca^{2+}-activated K^+ conductance; g_{Ca}, high-threshold Ca^{2+} conductance; and g_{sAHP}, slow Ca^{2+}-activated K^+ conductance. (**b**) Model reproduced the attention-dependent reduction in burstiness seen in our V4 neurons, as shown by the reduction in the peak of the normalized autocorrelation function in the attended condition relative to the unattended condition. (**c**) Model prediction of an attention-dependent reduction in extracellular action-potential height. Note the predicted spike-independent reduction in height, reflected in the downward shift of spike height curve when attention was directed into the RF. Shading indicates ± 1 s.e.m. Inset, attention-dependent reduction in action-potential height for matched levels of sodium inactivation. Extracellular action-potential is plotted as a function of the sodium inactivation variable, h, 0.6 ms before the peak of the action potential. h corresponds to the probability that the sodium inactivation particle is not blocking the channel. When h was large, more sodium channels were available to participate in the action potential, leading to spikes of higher amplitude. In addition to this dependence of spike height on sodium-channel inactivation ($P < 0.0001$ (Spearman's rank correlation), $R_s = 0.96$ attended, $R_s = 0.95$ unattended), the modeled predicted an attention-dependent reduction in spike height. This can be seen by the vertical shift between the height in the unattended condition and the attended condition.

as fluctuating excitatory and inhibitory conductances, representing synaptic inputs summed across populations of 'Poisson-spiking' inhibitory and excitatory neurons[23]. We assumed that attention proportionally increased both excitatory and inhibitory conductances, consistent with evidence that spatial attention increases activity among both pyramidal and inhibitory neurons[12], and with the normalization model of attention, which posits that attention increases the activity of both excitatory and inhibitory neurons[11,24].

In the model, attention-dependent increases in excitatory and inhibitory synaptic conductances caused a net depolarization, which resulted in an attention-dependent increase in firing rate. Depolarization also activated the muscarine-sensitive potassium channel, which has been shown to reduce burst firing in pyramidal neurons[20,21,25]. The attention-dependent increase in model input conductances gave rise to a reduction in burstiness that was comparable to what we observed experimentally (**Fig. 2b**; compare with **Fig. 1c**,**d**). At the same time, model neuron's firing rate increased from 27.4 Hz to 39.9 Hz, a gain change within the physiological range we observed. The model thus offers a simple, unified explanation for attention-dependent increases in firing rate and reductions in burst rate.

The voltage-dependent muscarine-sensitive potassium channel in our model was directly activated by depolarization. This led to the prediction that even after periods of time in which no spiking occurred, attentional modulation of subthreshold depolarization should reduce the neuron's propensity to burst. To test this, we examined whether attention modulated the burstiness of neurons after periods of neuronal silence. As the firing rates during these periods were identically zero, mechanisms that modulate burst firing by varying spike rate would not be expected to yield a change in the neuron's propensity to burst. For each neuron, we identified spikes that were preceded by 200 ms of silence and then calculated the difference in the percentage of ISIs <4 ms across the two attention conditions, normalized by their sum. Among the broad-spiking neurons, we found a significant reduction in this measure of burstiness with attention (Wilcoxon signed-rank test, $P = 0.0061$).

We also compared, on a cell-by-cell basis, the strength of the attention-dependent reduction of this measure across all time periods versus periods following at least 200 ms of quiescence, by computing the difference of these measures divided by their sum. If spike-dependent mechanisms were essential in this reduction, we would expect a decrease in the strength of this modulation after periods without spiking activity. Instead, we found a significant enhancement in this attention-dependent modulation of burstiness during quiescent periods (median −0.029 across all times versus −0.094 after silence; Wilcoxon signed-rank test, $P < 0.0001$), arguing against a spike-dependent mechanism. This result is consistent with our proposal, in which subthreshold depolarization is sufficient to yield reduction of burst firing.

In addition to providing a simple explanation for these two forms of attentional modulation, the model made the novel prediction of an attention-dependent reduction in action-potential height (**Fig. 2c**). This is illustrated in **Figure 2c**, which shows the model neuron's extracellular action-potential amplitude as a function of preceding ISI (preISI). In both attention conditions, the model predicted a reduction in action-potential height for spikes immediately after a prior action potential. This activity-dependent reduction in action-potential height arose from the inactivation of Na^+ channels caused by the depolarization during the preceding action potential, consistent with the findings of intracellular studies[26–29]. In addition to this spike history–dependent effect, the model made the prediction of an additional decrease in action-potential height with attention. In **Figure 2c**, this additional reduction is reflected in the downward shift of spike-height curve when attention was directed into the RF. This reduction in spike amplitude resulted, in part, from additional inactivation of sodium channels stemming from increased depolarization with attention. However, we also observed a reduction in height that was independent of sodium-channel inactivation (**Fig. 2c**). This reduction reflected increased excitatory and inhibitory conductances, which drove the neuron toward the excitatory and inhibitory reversal potentials, which are both below the maximum depolarization state reached during action-potential generation.

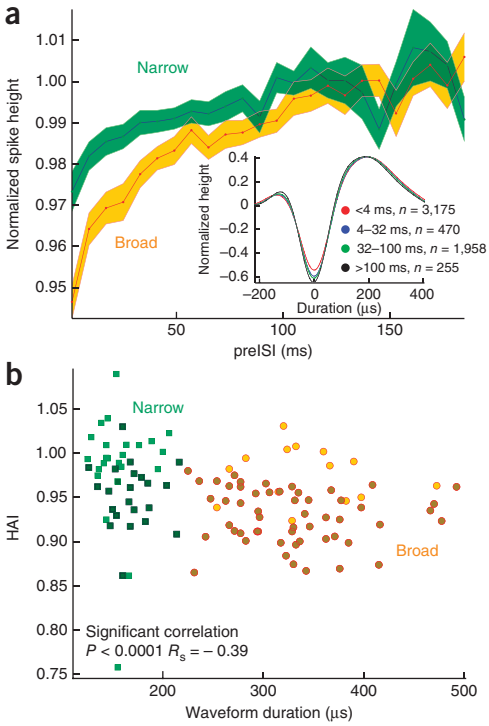

Figure 3 Narrow-spiking neurons show less spike history–dependent height adaptation than do broad-spiking neurons. (**a**) Time course of height adaptation among narrow- and broad-spiking neurons. Green and yellow lines show population average spike heights for narrow and broad-spiking populations, normalized to the unadapted spike height. Shaded regions correspond to ± 1 s.e.m. around the population means; bin size, 8 ms. Inset, spike history dependence of action-potential shape for an individual neuron. Each trace corresponds to the mean waveform of all action potentials evoked by the example neuron during the sustained period of the stimulus-evoked response, following the ISI (preISI) indicated in the legend. Spike amplitudes were all normalized to the amplitude of largely unadapted spikes preceded by ISIs > 100 ms. Spike amplitudes grew increasingly reduced at shorter preISIs. Thin shaded regions correspond to ± 1 s.e.m. of the interpolated waveform traces. (**b**) Significant correlation between mean waveform duration and spike HAI (Spearman's rank correlation, $P < 0.0001$, $R_s = -0.39$). For each neuron, the height adaptation index was computed by taking the mean normalized height of all action potentials with short preISIs (<4 ms). Narrow spiking neurons' action potentials (green squares, $n = 43$) were less adapted than broad-spiking neurons (orange circles, $n = 69$). Darker symbols correspond to neurons with significant height adaptation ($P < 0.001$). The difference between height adaptation among narrow-spiking and broad-spiking neurons was significant (Mann-Whitney U test, $P < 0.0001$).

Action potential shape depends on spike history

To test these predictions, we measured action potentials of each neuron as a function of preceding ISI and attention condition. We first considered whether we would observe the activity-dependent reduction in spike height predicted by the model, which to our knowledge had not been examined in the awake primate. As we observed for an example V4 neuron (**Fig. 3a**), action potentials were reduced in amplitude as the ISI decreased. Here we normalized spike height (voltage difference from peak to trough) by the mean height of the action potentials that were preceded by long ISIs (>100 ms) and were therefore largely unadapted. For each neuron, we then computed a height-adaptation index (HAI), defined as the mean normalized height of all action potentials with short preISIs (<4 ms). For the example neuron shown in **Figure 3a**, the HAI was 0.87, which corresponded to a 13% decrease in the height of action potentials that were preceded within 4 ms by another spike, which was highly significant (Wilcoxon signed-rank test, $P << 0.0001$). The effect of spike history–dependent adaptation was also highly significant across the population: the distribution of HAIs was significantly less than one (Wilcoxon signed-rank test, $P << 0.0001$), and 74/112 neurons (66.3%) exhibited individually significant height adaptation (Wilcoxon signed-rank test, $P < 0.001$; 52/67 (77.6%) broad-spiking neurons (2 excluded) and 22/43 (51.2%) narrow-spiking neurons).

Two classes of neurons can be distinguished in area V4, based on the duration of their action potentials: narrow-spiking neurons (putative fast-spiking inhibitory interneurons) and broad-spiking neurons (putative pyramidal neurons)[12]. Intracellular studies have found minimal height adaptation among fast-spiking inhibitory interneurons[28,30,31]. If narrow-spiking neurons largely correspond to fast-spiking inhibitory interneurons, they should therefore exhibit less spike-height adaptation than do broad-spiking neurons. Consistent with this hypothesis, V4 broad-spiking neurons had significantly stronger spike history–dependent height reduction than did narrow-spiking neurons (Mann-Whitney U test, $P < 0.0001$; median HAI: 0.9336 (broad-spiking neurons) and 0.9726 (narrow-spiking neurons)). The broad-spiking neurons also exhibited stronger reductions in action-potential height than did narrow-spiking neurons, as a function of ISI (**Fig. 3a**). In intracellular studies, this reduced adaptation among fast-spiking inhibitory interneurons has been shown to arise largely from the short duration of their action potentials, which results in fewer inactivated sodium channels[32]. Consistent with this finding, we also observed a significant correlation between HAI and mean action-potential duration, with broader neurons exhibiting stronger reductions in spike height (**Fig. 3b**; Spearman's rank correlation, $P < 0.0001$ $R_s = -0.39$).

Attention-dependent reductions in action-potential height

As predicted by our model, we found a small reduction in action-potential height with attention. We show this for an example broad-spiking neuron (**Fig. 4a**). Consistent with the model prediction, action potentials elicited in the unattended condition were consistently larger in amplitude than those elicited in the attended condition, across matched preISI bins. To examine the distribution of this attention effect across the population, we computed an attention height index (AHI), which quantified the change in spike height when attention was directed into the RF. The AHI was computed by taking the mean (across preISI bins) of: (normalized attended height − normalized unattended height)/(normalized attended height + normalized unattended height). Across the population, the distribution was significantly less than zero, corresponding to a reduction in action-potential height with attention (Wilcoxon signed-rank test; entire population, median AHI = −0.0034, $P = 0.00063$; broad −0.0033, $P = 0.019$; narrow −0.0035, $P = 0.0041$).

The proposed model predicted that spike height would be reduced by two distinct attention-dependent mechanisms, and we observed evidence for both. First, attention was assumed to increase synaptic conductances. These conductances, as well as voltage-gated conductances they activate, were predicted to reduce action-potential height. This is because their reversal potentials are hyperpolarized, relative to the peak depolarization reached during the action potential. As a result, an increase in synaptic conductances would cause an increase in hyperpolarizing currents, which in turn would reduce action-potential amplitude[33]. In addition, the model predicted that an increase in firing rate would add to this reduction in spike amplitude. This is because each action potential would inactivate sodium channels, which deinactivate over time. During this recovery period, fewer

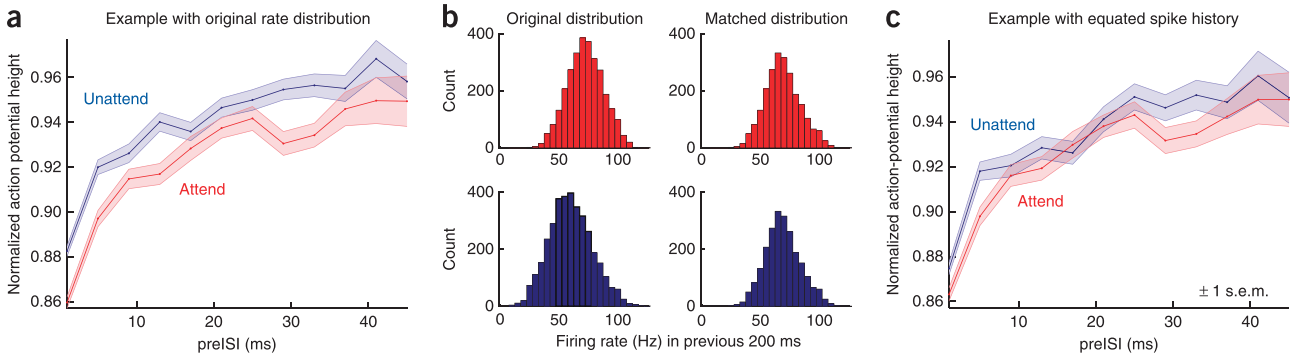

Figure 4 Attention-dependent reduction in action-potential height. (**a**) Action potentials elicited in the attended and unattended condition, across matched preISI bins. Shaded regions correspond to ± 1 s.e.m.; bin size, 4 ms. (**b**) Method for equating recent spike history across attention conditions, for the example neuron shown in **a**. Firing rates during the 200-ms period preceding each spike in the attend RF (red) and attend away (blue) conditions (left). The distribution was shifted to the right with attention because firing rates were higher with attention. To equate spike history across attention conditions, within each bin, we randomly discarded spikes from whichever attention condition had more spikes. This allowed us to compare action potentials that were matched in preceding spike history. Distributions of spike counts, equated across attention conditions, after applying this spike-history matching procedure, to control for differences in spike history–dependent adaptation are shown on the right. (**c**) Action-potential height after the application of the spike-history–matching procedure illustrated in **b**.

channels would be available to contribute to the next action potential, reducing its amplitude. This phenomenon is known as spike-height adaptation. Increasing firing rate would reduce the average ISI, causing more spikes to fall within this adaptation window. As attention increases firing rate, the model predicted that in addition to any reduction in action-potential amplitude caused by increases in synaptic conductance, attention would also reduce action-potential height indirectly, via an increase in spike-height adaptation.

To test the model, it was therefore essential to isolate these two hypothesized sources of attention-dependent reduction in spike amplitude. To control for spike history–dependent adaptation, we used several methods designed to equate action-potential history across attention conditions. Spike history–dependent adaptation occurs over relatively short time periods (**Figs. 2c** and **3a**). Therefore, we conducted control analyses designed to equate the number of spikes within this adaptation window, across attention conditions. We used 200 ms as a conservative estimate of the spike-adaptation window, which we chose to exceed the period over which we observed action potentials to recover from the adaptation caused by the prior spike (**Fig. 3a**). First, we counted the number of spikes that preceded each action potential in a 200-ms adaptation window (**Fig. 4b**). The distribution of firing rates falling within the adaptation window during each attention condition shifted to the right with attention, because firing rates were higher with attention. We then equated spike history across attention conditions, as follows. Within each bin, we randomly discarded spikes from whichever attention condition had more spikes, which matched the spike-history distribution across the two attention conditions (**Fig. 4b**). After equating recent spike history in this manner, we continued to find a significant attention-dependent reduction in AHI, both for the example neuron (**Fig. 4c**), and across the population (Wilcoxon signed-rank test, $P = 0.0044$). Reductions in AHI were significant in each monkey ($P < 0.05$). Within the 200-ms adaptation window, additional spikes occurring within shorter intervals would be expected to contribute more to spike-height reduction than spikes occurring at longer intervals. We thus repeated the analysis to equate spike count over shorter periods of adaptation 10 ms, 25 ms, 50 ms and 100 ms. We found that the reduction in spike height was significant (Wilcoxon signed-rank test, $P < 0.05$) across all windows.

The above analysis equated spike count across the prespike period over which we observed measurable spike history–dependent adaptation. However, it is possible that differences in mean firing rate could have contributed to spike-height adaptation over longer time periods. We controlled for this by recomputing the AHI over trials that were matched in firing rate across attention conditions. First, we counted the number of action potentials that occurred when the attended or unattended stimulus paused with the RF. We then selected trials with matched numbers of spike counts in both attention conditions. As we frequently had more trials with a given spike count in one attention condition than the other, we randomly discarded trials from the more numerous condition until the number of trials at each spike count was identical across attention conditions. We repeated this for all observed spike counts, thereby identically matching spike-count distributions across attention conditions. We then computed the AHI from the resulting rate-matched trials. For each neuron, we repeated this random selection process 100 times and averaged the resulting trial-matched AHI data. After matching rates in this manner, we found that action-potential heights were still significantly reduced in magnitude (one-tailed Wilcoxon signed-rank test, $P = 0.023$; median AHI of −0.0016). As a final test, we combined the two controls. First, we performed the rate-matching procedure to exactly match firing rates across the two attention conditions. After selecting this rate-matched subset of trials, we then equated recent spike history by selecting from these trials subsets of action potentials that were exactly matched in the number of preceding spikes in a 200-ms spike-adaptation window. After performing this combined firing-rate and spike-history control, we found that action-potential height was significantly reduced by attention (one-tailed Wilcoxon signed-rank test, $P = 0.023$, median AHI −0.0021). We repeated this analysis across the full range of spike-adaptation windows. For all windows, spike height was significantly reduced by attention ($P < 0.05$, one-tailed Wilcoxon signed-rank test, for bins of 10 ms, 25 ms, 50 ms, 100 ms and 200 ms). We thus conclude that, after accounting for differences in spike history–dependent adaptation, attention reduced action-potential height, as predicted by the model.

DISCUSSION

The present study advances our understanding of the neural mechanisms underlying attention in several ways. It provides the first evidence for an attention-dependent modulation of burstiness. The observed reduction in burstiness with attention contradicts the

widely held view that bursts are a privileged communication channel. If bursts conveyed information with greater fidelity than isolated spikes, we would expect bursts to increase when stimuli are task-relevant and attention is directed toward them. The reduction in burst firing is instead consistent with the view that bursts are a source of response variability that is reduced so as to improve neuronal signaling of attended stimuli. Burst firing has also been implicated in other aspects of cortical computation, including plasticity[8,9], synaptic integration[1,9] and communication to select subpopulations[7]. Thus the attention-dependent changes in burst firing observed in the current study are likely to have important consequences for these aspects of cortical computation.

One previous study examined attentional modulation of burst firing and did not find evidence for a change[34]. That study measured the raw rate of spikes with short ISIs. This would be expected to increase with attention-dependent increases in firing rate, potentially masking a reduction in burst firing. Indeed, when we applied the metric used in that study[34], we did not detect a reduction. They[34] also examined the relationship between raw burst rate and firing rate across neurons, which is less sensitive than the within-cell comparison we used here. We did not detect the observed reduction in burst firing when we applied this second metric. Thus, although the conclusions of the two studies differ, the difference likely stems from differences in the sensitivity of the analyses adopted.

To account for this attention-dependent reduction in burstiness, we developed the scaled conductance model of attention. This model was inspired by a previous model where burst firing depends, in part, on the interaction between voltage-gated muscarinic potassium conductances and fast persistent sodium channels[22]. Our model posited that attention-dependent increases in depolarization activate these muscarinic channels, reducing burst firing. This proposal is consistent with the finding that cortical pyramidal neurons become less bursty when they are depolarized[20,21]. Burstiness has also been found to be reduced with elevated levels of arousal[21]. The present findings thus support the hypothesis that mechanisms of selective attention are shared, in part, with those mediating changes in arousal[35]. We hypothesize that attention and arousal have in common an increase in depolarization that, in the case of selective attention, is mediated by spatially selective feedback signals, such as those generated by the oculomotor system[36].

Alternative models of burst firing, such as 'ping-pong' models that incorporate back-propagation of action potentials between somatic and dendritic compartments[37–39], could also potentially account for our findings. However, we observed significant attention-dependent reductions in burstiness that were undiminished after periods of silence. Thus, differences in spiking activity are not necessary to generate the observed reduction in burstiness. This argues against the necessity of the spike-dependent burst mechanism featured in these models to account for reductions in burstiness. Rather, we propose that attention-dependent reductions in burst firing result from periods of heightened subthreshold depolarization. Though technically difficult, this prediction could be tested directly using intracellular recording methods in monkeys during the performance of attention-demanding tasks[40].

In the scaled conductance model of attention, attention increases excitation and inhibition in tandem. This is not strictly necessary: attention-dependent reduction in spike height and the reduction in burst firing can be observed in a model in which only excitatory conductances are increased. However, conjoint increases in inhibitory conductances (whose reversal potentials are more hyperpolarized than are excitatory conductances) did contribute strongly in the model to spike height reduction and helped keep the attention-dependent increase in spike rate in the experimentally observed range. The assumption that increases in excitation are accompanied by increases in inhibition is also consistent with experiments showing that changes in excitation are often found to be accompanied by corresponding changes in inhibition, as might be expected from the fact that excitatory neurons drive inhibitory neurons[41]. It is further supported by the finding that attention causes increases in the firing rates of both broad-spiking (putative excitatory) and narrow-spiking (putative inhibitory) neurons[12].

The second innovation in our study was the use of the extracellular action-potential shape, coupled with conductance-based models to provide a 'window' into the state variables that modulate spike amplitude[26–31,42]. Although a few studies have examined changes in extracellular action-potential height in the rat[42–45] this is, to our knowledge, the first study in the nonhuman primate to use changes in spike shape to make inferences about neural mechanisms underlying changes in cognitive state. Specifically, our model made the novel prediction of an attention-dependent reduction in action-potential height. Consistent with this, we found a small yet measurable attention-dependent reduction in action-potential height among both broad and narrow-spiking V4 neurons. Not only does this finding link a very-low level phenomenon, action-potential shape, to a high-level phenomenon, attention, it is a specific and surprising prediction of the proposed model, which is the first channel-level model of attention to be tested empirically. This study therefore takes an important step toward the longstanding goal of achieving a mechanistic, reductionist understanding of attention.

METHODS

Methods and any associated references are available in the online version of the paper.

Note: Supplementary information is available in the online version of the paper.

ACKNOWLEDGMENTS

This work was supported in part by US National Eye Institute grant EY13802 (J.F.M. and J.H.R.) and The Gatsby Charitable Foundation (E.B.A. and J.H.R.). We thank K. Sundberg for help in data collection, and C. Williams and J. Reyes for help with animal care.

AUTHOR CONTRIBUTIONS

E.B.A. analyzed the data and built the model. J.F.M. collected most of the physiology data and contributed to the burst-reduction analyses. E.B.A., J.F.M. and J.H.R. wrote the manuscript.

COMPETING FINANCIAL INTERESTS

The authors declare no competing financial interests.

1. Krahe, R. & Gabbiani, F. Burst firing in sensory systems. *Nat. Rev. Neurosci.* **5**, 13–23 (2004).
2. Sherman, S.M. Tonic and burst firing: dual modes of thalamocortical relay. *Trends Neurosci.* **24**, 122–126 (2001).
3. Cattaneo, A., Maffei, L. & Morrone, C. Patterns in the discharge of simple and complex visual cortical cells. *Proc. R. Soc. Lond. B Biol. Sci.* **212**, 279–297 (1981).
4. Samonds, J.M. & Bonds, A.B. From another angle: differences in cortical coding between fine and coarse discrimination of orientation. *J. Neurophysiol.* **91**, 1193–1202 (2004).
5. Shih, J.Y., Atencio, C.A. & Schreiner, C.E. Improved stimulus representation by short interspike intervals in primary auditory cortex. *J. Neurophysiol.* **105**, 1908–1917 (2011).
6. Reich, D.S., Mechler, F., Purpura, K.P. & Victor, J.D. Interspike intervals, receptive fields, and information encoding in primary visual cortex. *J. Neurosci.* **20**, 1964–1974 (2000).

7. Izhikevich, E.M., Desai, N.S., Walcott, E.C. & Hoppensteadt, F.C. Bursts as a unit of neural information: selective communication via resonance. *Trends Neurosci.* **26**, 161–167 (2003).
8. Caporale, N. & Dan, Y. Spike timing-dependent plasticity: a Hebbian learning rule. *Annu. Rev. Neurosci.* **31**, 25–46 (2008).
9. Sjöström, P.J., Rancz, E.A., Roth, A. & Häusser, M. Dendritic excitability and synaptic plasticity. *Physiol. Rev.* **88**, 769–840 (2008).
10. De Weerd, P., Peralta, M.R. III, Desimone, R. & Ungerleider, L.G. Loss of attentional stimulus selection after extrastriate cortical lesions in macaques. *Nat. Neurosci.* **2**, 753–758 (1999).
11. Reynolds, J.H. & Heeger, D.J. The normalization model of attention. *Neuron* **61**, 168–185 (2009).
12. Mitchell, J.F., Sundberg, K.A. & Reynolds, J.H. Differential attention-dependent response modulation across cell classes in macaque visual area V4. *Neuron* **55**, 131–141 (2007).
13. Brumberg, J.C., Nowak, L.G. & McCormick, D.A. Ionic mechanisms underlying repetitive high-frequency burst firing in supragranular cortical neurons. *J. Neurosci.* **20**, 4829–4843 (2000).
14. Nowak, L.G., Azouz, R., Sanchez-Vives, M.V., Gray, C.M. & McCormick, D.A. Electrophysiological classes of cat primary visual cortical neurons *in vivo* as revealed by quantitative analyses. *J. Neurophysiol.* **89**, 1541–1566 (2003).
15. Vigneswaran, G., Kraskov, A. & Lemon, R.N. Large identified pyramidal cells in macaque motor and premotor cortex exhibit "thin spikes": implications for cell type classification. *J. Neurosci.* **31**, 14235–14242 (2011).
16. Anderson, E.B., Mitchell, J.F. & Reynolds, J.H. Attentional modulation of firing rate varies with burstiness across putative pyramidal neurons in macaque visual Area V4. *J. Neurosci.* **31**, 10983–10992 (2011).
17. Mitchell, J.F., Sundberg, K.A. & Reynolds, J.H. Spatial attention decorrelates intrinsic activity fluctuations in macaque area V4. *Neuron* **63**, 879–888 (2009).
18. Arieli, A., Sterkin, A., Grinvald, A. & Aertsen, A. Dynamics of ongoing activity: explanation of the large variability in evoked cortical responses. *Science* **273**, 1868–1871 (1996).
19. Smith, M.A. & Kohn, A. Spatial and temporal scales of neuronal correlation in primary visual cortex. *J. Neurosci.* **28**, 12591–12603 (2008).
20. Wang, Z. & McCormick, D.A. Control of firing mode of corticotectal and corticopontine layer V burst-generating neurons by norepinephrine, acetylcholine, and 1S,3R-ACPD. *J. Neurosci.* **13**, 2199–2216 (1993).
21. Steriade, M., Timofeev, I. & Grenier, F. Natural waking and sleep states: a view from inside neocortical neurons. *J. Neurophysiol.* **85**, 1969–1985 (2001).
22. Golomb, D., Cuiyong, Y. & Yaari, Y. Contribution of persistent Na+ current and M-type K+ current to somatic bursting in CA1 pyramidal cells: combined experimental and modeling study. *J. Neurophysiol.* **96**, 1912–1926 (2006).
23. Destexhe, A., Rudolph, M., Fellous, J.M. & Sejnowski, T.J. Fluctuating synaptic conductances recreate *in vivo*-like activity in neocortical neurons. *Neuroscience* **107**, 13–24 (2001).
24. Reynolds, J.H., Chelazzi, L. & Desimone, R. Competitive Mechanisms Subserve Attention in Macaque Areas V2 and V4. *J. Neurosci.* **19**, 1736–1753 (1999).
25. Yue, C. & Yaari, Y. KCNQ/M channels control spike afterdepolarization and burst generation in hippocampal neurons. *J. Neurosci.* **24**, 4614–4624 (2004).
26. Colbert, C.M., Magee, J.C., Hoffman, D.A. & Johnston, D. Slow recovery from inactivation of Na+ channels underlies the activity-dependent attenuation of dendritic action potentials in hippocampal CA1 pyramidal neurons. *J. Neurosci.* **17**, 6512–6521 (1997).
27. Jung, H.-Y., Mickus, T. & Spruston, N. Prolonged sodium channel inactivation contributes to dendritic action potential attenuation in hippocampal pyramidal neurons. *J. Neurosci.* **17**, 6639–6646 (1997).
28. Martina, M. & Jonas, P. Functional differences in Na^+ channel gating between fast-spiking interneurones and principal neurones of rat hippocampus. *J. Physiol. (Lond.)* **505**, 593–603 (1997).
29. Bean, B.P. The action potential in mammalian central neurons. *Nat. Rev. Neurosci.* **8**, 451–465 (2007).
30. McCormick, D.A., Connors, B.W., Lighthall, J.W. & Prince, D.A. Comparative electrophysiology of pyramidal and sparsely spiny neurons of the neocortex. *J. Neurophysiol.* **54**, 782–806 (1985).
31. Gonzàlez-Burgos, G., Krimer, L.S., Povysheva, N.V., Barrionuevo, G. & Lewis, D.A. Functional properties of fast spiking interneurons and their synaptic connections with pyramidal cells in primate dorsolateral prefrontal cortex. *J. Neurophysiol.* **93**, 942–953 (2005).
32. Carter, B.C. & Bean, B.P. Sodium entry during action potentials of mammalian neurons: incomplete inactivation and reduced metabolic efficiency in fast spiking neurons. *Neuron* **64**, 898–909 (2009).
33. de Polavieja, G.G., Harsch, A., Kleppe, I., Robinson, H.P.C. & Juusola, M. Stimulus history reliably shapes action potential waveforms of cortical neurons. *J. Neurosci.* **25**, 5657–5665 (2005).
34. McAdams, C.J. & Maunsell, J.H. Effects of attention on orientation tuning functions of single neurons in macaque cortical area V4. *J. Neurosci.* **19**, 431–441 (1999).
35. Harris, K.D. & Thiele, A. Cortical state and attention. *Nat. Rev. Neurosci.* **12**, 509–523 (2011).
36. Noudoost, B., Chang, M.H., Steinmetz, N.A. & Moore, T. Top-down control of visual attention. *Curr. Opin. Neurobiol.* **20**, 183–190 (2010).
37. Pinsky, P.F. & Rinzel, J. Intrinsic and network rhythmogenesis in a reduced traub model for CA3 neurons. *J. Comp. Neurosci.* **1**, 39–60 (1994).
38. Mainen, Z.F. & Sejnowski, T.J. Influence of dendritic structure on firing pattern in model neocortical neurons. *Nature* **382**, 363–366 (1996).
39. Kepecs, A. & Wang, X.-J. Analysis of complex bursting in cortical pyramidal neuron models. *Neurocomputing* **32**, 181–187 (2000).
40. Matsumura, M., Chen, D., Sawaguchi, T., Kubota, K. & Fetz, E.E. Synaptic interactions between primate precentral cortex neurons revealed by spike-triggered averaging of intracellular membrane potentials *in vivo*. *J. Neurosci.* **16**, 7757–7767 (1996).
41. Anderson, J.S., Carandini, M. & Ferster, X. Orientation tuning of input conductance, excitation and inhibition in cat primary visual cortex. *J. Neurophysiol.* **84**, 909–926 (2000).
42. Gold, C., Henze, D.A., Koch, C. & Buzsáki, G. On the origin of the extracellular action potential waveform: a modeling study. *J. Neurophysiol.* **95**, 3113–3128 (2006).
43. Henze, D.A. *et al.* Intracellular features predicted by extracellular recordings in the hippocampus *in vivo*. *J. Neurophysiol.* **84**, 390–400 (2000).
44. Harris, K.D. *et al.* Temporal interaction between single spikes and complex spike bursts in hippocampal pyramidal cells. *Neuron* **32**, 141–149 (2001).
45. Quirk, M.C., Blum, K.E. & Wilson, M.A. Experience-dependent changes in extracellular spike amplitude may reflect regulation of dendritic action potential back-propagation in rat hippocampal pyramidal cells. *J. Neurosci.* **21**, 240–248 (2001).

ONLINE METHODS

Statistical analysis. Nonparametric tests were used to avoid assumptions inherent in parametric tests. *P* values are reported for each test, except where multiple tests were performed and the results in each were significant at the $P < 0.05$ level. *P* values greater than 0.0001 have been rounded to two significant digits. No statistical tests were run to determine sample size a priori. The sizes we chose are similar to those used in previous publications.

Electrophysiology and receptive field characterization. All procedures were approved by the Salk Institute Institutional Animal Care and Use Committee and conformed to US National Institutes of Health guidelines for the humane care and use of animals in research. Monkeys were prepared for neuronal recording following procedures as described previously[12]. Recordings were made from tungsten electrodes (FHC) that were advanced until action potentials of single neurons could be isolated based on action-potential waveform shape. Neuronal signals were recorded extracellularly, filtered (Butterworth filter, 6-pole, 3-db cutoffs at 154 Hz and 8.8 kHz), and stored using the Multichannel Acquisition Processor system (Plexon, Inc.). Spike waveforms crossing a negative threshold, which was set to exclude noise, were stored for later off-line analysis. Units were identified as isolated in offline analysis (Offline Sorter, Plexon, Inc.) if the first three principal components of their waveform shape formed a clearly separable cluster from noise and other units. After isolating one or more neurons, RFs were mapped using a subspace reverse correlation procedure[12,46]. In this procedure, Gabor stimuli (eight orientations, six colors, 80% luminance contrast, 1.2 cycles per degree, Gabor Gaussian half-width, 2°) were flashed to determine a single stimulus location that would elicit a robust visual response. When multiple neurons were recorded simultaneously, the features and location of the stimulus were selected to excite the best-isolated units.

Stimulus presentation and eye movement monitoring. Stimuli were presented on a computer monitor (Sony Trinitron Multiscan, TC, 640 × 480 pixel resolution, 120 Hz) placed 57 cm from the eye. Experimental control was handled by NIMH Cortex software.

Eye position was continuously monitored with an infrared eye tracking system (240 Hz, ETL-400; ISCAN, Inc.).

Task and stimuli. Two monkeys performed a multiple-object tracking task that has been used to study attention in humans[47,48] and nonhuman primates[12,16,17]. The monkeys began each trial by fixating a central point and maintained fixation until the end of the trial. After 200 ms, four identical Gabor stimuli appeared (40% luminance contrast). The color and orientation of these stimuli were chosen based on the subspace reverse correlation map to produce a strong response. The positions of the stimuli were selected to fall at regular intervals along an invisible ring of equal eccentricity, selected such that all of the stimuli fell outside of the neurons' RFs. One or two stimuli were then cued as targets by a brief elevation in luminance. All four stimuli then moved along independent, randomly generated trajectories that positioned the stimuli at four new, equally eccentric positions. This placed one of the stimuli at the center of the neuron's RF and the others outside the RF. The trajectories were designed to match stimulation history across the two attention conditions, by using the identical trajectories in the attended and unattended trials, and by preventing all but one stimulus from entering the RF. The stimuli then paused for 1,000 ms before moving to a final set of equally eccentric positions and stopping. At this point, the fixation point disappeared, signaling the monkey to make a saccade to each cued target. To minimize the development of spatial biases, the starting and ending positions for the target and nontarget stimuli were symmetrically balanced. Correct identification of the targets resulted in a liquid reward.

Measurement of action-potential shape. Action potential waveforms were obtained from the Plexon Multichannel Acquisition Processor system, which digitized the waveforms to 25 μs. To calculate the height of an action potential, we subtracted the trough from the peak of the waveform. To calculate waveform duration, we spline-interpolated the waveforms from 25 μs to a resolution of 0.05 μs and then calculated the time from the trough to the peak[12]. We then normalized these measures by the mean height or duration of action potentials in the stimulus-free fixation period to reduce the effects of long-timescale drift in action-potential shape (**Supplementary Fig. 3**). Two broad-spiking neurons did not have any action potentials with a preISI < 4 ms and were excluded from HAI analyses.

Broad-spiking and narrow-spiking classification. As described previously[12], we divided neurons into narrow-spiking and broad-spiking subpopulations based on waveform duration. We defined waveform duration to be the time from the trough to the peak of the average waveform[12]. We selected this metric on the basis of studies showing that this measure best distinguishes putative pyramidal neurons from putative fast-spiking interneurons in the neocortex[49]. The distribution of spike-waveform duration was significantly bimodal across all isolated cells with biphasic spike waveforms ($n = 202$, Hartigan's dip test, $P < 0.0001$), and also across the subset of these cells with significant visual responses ($n = 118$, Hartigan's dip test, $P < 0.01$). Narrow- and broad-spiking neurons were separated based on the trough between the two modes of the waveform duration distribution, with narrow-spiking neurons defined as those ranging in duration from 120 μs to 224 μs and broad-spiking neurons defined as those ranging in duration from 225 μs to 500 μs.

Inclusion criteria. We recorded from 206 well-isolated neurons from two male adult macaques ($n = 53$ monkey B, $n = 153$ monkey M). We restricted our discharge pattern analyses to units whose response on trials when attention was directed away from the RF exceeded 5 Hz, averaged over the final 500 ms of the stimulus pause period and was significantly greater than the mean spontaneous firing rate averaged over the 250 ms before the onset of the Gabor stimuli (Mann-Whitney *U* test, $P < 0.05$). This resulted in 84 neurons being excluded. In addition, four units were excluded because their waveforms did not have the typical biphasic shape, with a trough followed by a clearly defined peak, and they could not therefore be classified as narrow-spiking or broad-spiking. This resulted in 118 neurons that met these selection criteria. For the waveform adaptation analyses, we excluded six additional neurons, resulting in 112 neurons. Two of these were excluded because only mean waveform data were available, and the other four were excluded as the peak of many of their waveforms could not be determined. Unless otherwise specified, analysis of spiking statistics was restricted to the final 800 ms of the pause period (the 'sustained period'), which excluded periods of transient response as stimuli entered or exited the RF, and thus the mean firing rate was relatively stationary.

Burst analysis. We computed two burst measures: an ISI-based metric that calculated the percentage of ISIs < 4 ms, and an autocorrelation function–based metric. For the second measure, we calculated the autocorrelation function of the neuron separately for each attention condition for the correct two of four tracking trials. We then subtracted the shuffle predictor for that condition. The shuffle predictor is defined as the mean cross-correlation across all pairs of trials of an individual neuron. By subtracting the predictor, we removed any trial-locked fluctuations in spiking that result from repeated presentation of the stimulus. After this subtraction, we normalized the result by the shuffle predictor at each time lag. This defined the normalized autocorrelation function, depicted for example neurons in **Figure 1c**,**d**. To further isolate changes in burst firing from changes in low-frequency fluctuations in firing rate, we defined a filter that served to eliminate contributions to the autocorrelation from rate fluctuations below 10 Hz, the range where we have previously reported shared fluctuations in firing rate over the neuronal population[17]. It was created by taking the inverse fast Fourier transform of the following equation:

$$\text{if freq} < 22.5, \text{ then } \left(1 + e^{\frac{-(\text{freq} - 11.5)}{0.75}}\right)^{-1}$$

$$\text{otherwise } \left(1 + e^{\frac{+(\text{freq} - 33.5)}{0.75}}\right)^{-1}$$

The burstiness index (BI) was computed as the sum of the product of the described filter with normalized autocorrelation defined above. As an additional control analysis to further isolate attention-dependent reductions in burst firing from slow fluctuations, we also applied a spike-jitter analysis (**Supplementary Fig. 4**)[19].

doi:10.1038/nn.3463

Single compartment model. We implemented the Golomb single-compartment model described in previous work[22]. A schematic of the model can be seen in **Figure 2a**. The model was implemented using Matlab software (Mathworks) with a temporal resolution of 0.02 ms, and was constructed of coupled differential equations according to a Hodgkin-Huxley–type scheme. The model includes many of the currents known to exist in the soma and proximal dendrites of pyramidal neurons, including the transient Na^+ current (I_{Na}) the delayed rectifier K^+ current (I_{Kdr}) that generate spikes. In the original paper[22], the authors use a fast-slow analysis to demonstrate that bursting in the model arises from the interplay of the slow timescale of the muscarinic-sensitive K^+ current (I_M) and the fast timescale of the transient and persistent Na^+ currents (I_{Na} and I_{Nap})[22]. Just as varying the conductances of these currents varies the intrinsic burstiness of the model neuron, differences in expression of the persistent Na^+ channel may underlie some of the variability in burstiness seen across pyramidal neurons in different cortical layers[50].

Although these four currents are sufficient to give rise to most of the model behavior, we included the other currents found in the full nonzero $[Ca^{2+}]$ Golomb model[22]. This includes an A-type K^+ current (I_A), the high-threshold Ca^{2+} current (I_{Ca}), and two Ca^{2+} activated K^+ currents: the fast Ca^{2+}-activated K^+ current (I_{Kca}), which contribute to rapid spike repolarization and the slow Ca^{2+}-activated K^+ current (I_{sAHP}), which mediates a slow after-hyperpolarization and spike frequency adaptation. In total, the current balance equation is:

$$C\frac{dv}{dt} = -g_L(V - V_L) - I_{Na} - I_{Nap} - I_{Kdr} - I_M - I_A - I_{Ca} - I_{Kca} - I_{sANP} + I_{syn}$$

where $C = 1\ \mu F/cm^2$, $g_L = 0.05\ mS/cm^2$, $V_L = -70$ mV, and I_{syn} is the synaptic current (see below). The ionic currents are: $I_{Na}(V, h) = g_{Na}m_\infty^3(V)h(V - V_{Na})$, $I_{Nap}(V) = g_{Nap}p_\infty(V)(V - V_{Na})$, $I_{Kdr}(V, n) = g_{Kdr}n^4(V - V_K)$, $I_A(V, b) = g_A a_\infty^3(V)b(V - V_K)$, $I_M(V, z) = g_M z(V - V_K)$, $g_{Ca}r^2(V - V_{Ca})$, $I_{Kca}(V, c) = g_C d_\infty([Ca^{2+}]_i)c(V - V_K)$, $I_{sAHP}(V, q) = g_{sAHP}q(V - V_K)$. The reversal potentials are $V_{Na} = 55$ mV, $V_K = -90$ mV and $V_{Ca} = 120$ mV. All conductances are equal to or within the range of parameters used in the original paper[22]: $g_{Na} = 35\ mS/cm^2$, $g_{NaP} = 0.3\ mS/cm^2$, $g_{Kdr} = 6\ mS/cm^2$, $g_A = 1.4\ mS/cm^2$, $g_M = 1\ mS/cm^2$, $g_{Ca} = 0.02\ mS/cm^2$, $g_{Kca} = 10\ mS/cm^2$ and $g_{sAHP} = 5\ mS/cm^2$. The dynamics of calcium concentration inside the compartment are:

$$\frac{d[Ca^{2+}]}{dt} = -\nu I_{Ca} - \frac{[Ca^{2+}]}{\tau_{Ca}}$$

where $\nu = 0.13\ cm^2\ ms^{-1}\ \mu A^{-1}$, $\tau_{Ca} = 13$ ms. The kinetics equations are identical to those used in the original paper[15]. Extracellular action potentials were modeled as the first derivative of the intracellular voltage.

Synaptic input to model. To simulate conditions *in vivo*, we modified the Golomb model by replacing the applied current with a synaptic current, I_{syn} (**Fig. 2a**). This synaptic current was generated by a point-conductance model to approximate fluctuating synaptic activity seen *in vivo*[23]. This current is the sum of independent excitatory and inhibitory conductances, $g_e(t)$ and $g_i(t)$:

$$I_{syn} = g_e(t)(V - 0) + g_i(t)(V - 75)$$

Each of these conductances is described by one-variable stochastic processes similar to an Ornstein-Uhlenbeck process[23], and is equivalent to the sum of many Poisson processes smoothed by a synaptic time constant. The time constants for the excitatory and inhibitory conductances were 2.71 ms and 10.49 ms, respectively. The mean of the inhibitory conductance was twice as strong as the excitatory conductance, but we obtained qualitatively similar results when we varied the relative balance of these conductances.

To simulate attentional modulation, we scaled the synaptic inputs to the model. We accomplished this by proportionally increasing the means of the excitatory and inhibitory conductances by an attentional factor, A, and scaling the s.d. of these processes by the square root of A. By the central limit theorem, summing a large population of Poisson inputs results in a Gaussian random variable with a mean equal to the number of inputs and a variance that is proportional to the mean (s.d. proportional to the square root of the mean). Thus, the scaling applied here is equivalent to scaling of the rate parameters of a large population of Poisson synaptic inputs.

46. Ringach, D.L., Hawken, M.J. & Shapley, R. Dynamics of orientation tuning in macaque primary visual cortex. *Nature* **387**, 281–284 (1997).
47. Pylyshyn, Z.W. & Storm, R.W. Tracking multiple independent targets: evidence for a parallel tracking mechanism. *Spat. Vis.* **3**, 179–197 (1988).
48. Cavanagh, P. & Alvarez, G.A. Tracking multiple targets with multifocal attention. *Trends Cogn. Sci.* **9**, 349–354 (2005).
49. Barth, P. *et al.* Characterization of neocortical principal cells and interneurons by network interactions and extracellular features. *J. Neurophysiol.* **92**, 600–608 (2004).
50. Aracri, P. *et al.* Layer-specific properties of the persistent sodium current in sensorimotor cortex. *J. Neurophysiol.* **95**, 3460–3468 (2006).

Erratum: Attention-dependent reductions in burstiness and action-potential height in macaque area V4

Emily B Anderson, Jude F Mitchell & John H Reynolds
Nat. Neurosci.; **doi:10.1038/nn.3463; corrected online 17 July 2013**

In the version of this article initially published online, burstiness was defined on p. 1 as the prosperity of neurons to fire rather than the propensity, and model neuron firing rates were given on p. 3 in nHz rather than Hz. The errors have been corrected for the print, PDF and HTML versions of this article.